Bias-Independent Inter-Modulation Method for Simultaneously Measuring Low-Frequency Modulation and Bias Half-Wave Voltages of Mach-Zehnder Modulators

Junfeng ZHU†, Xinhai ZOU†, Ying XU, Yutong HE, Yali ZHANG, Zhiyao ZHANG, Shangjian ZHANG*, and Yong LIU

Advanced Research Center for Microwave Photonics (ARC-MWP), State Key Laboratory of Electronic Thin Films and Integrated Devices, School of Optoelectronic Science and Engineering, University of Electronic Science and Technology of China, Chengdu 611731, China

†*These authors contributed equally to this work and are both first authors*

*Corresponding author: Shangjian ZHANG E-mail: sjzhang@uestc.edu.cn

Abstract: A bias-independent inter-modulation method is proposed and demonstrated for measuring low-frequency modulation and bias half-wave voltages of Mach-Zehnder modulators (MZMs). The method consists of simultaneous sinusoidal modulation on the modulation and bias ports of the MZM under test. Sinusoidal-modulated sidebands heterodyne with each other and generate the desired inter-modulation products after photodetection, which allows extracting both the modulation depth and half-wave voltage for the modulation and bias ports of the MZM. Our method is independent of bias voltages of the MZM, which can be canceled out by carefully choosing the sinusoidal-modulation frequencies. Moreover, the proposed method enables the low swing voltage for measuring both the modulation depth and half-wave voltage of MZMs. Experiments indicate that the proposed method features the simple setup and high accuracy for low-frequency response measurement ranging from 1 Hz to 1 MHz.

Keywords: Electrooptical modulation; fiber optics systems; half-wave voltage; inter-modulation

Citation: Junfeng ZHU, Xinhai ZOU, Ying XU, Yutong HE, Yali ZHANG, Zhiyao ZHANG, *et al.*, "Bias-Independent Inter-Modulation Method for Simultaneously Measuring Low-Frequency Modulation and Bias Half-Wave Voltages of Mach-Zehnder Modulators," *Photonic Sensors*, 2023, 13(2): 230203.

1. Introduction

Electro-optic response parameters of the modulation depth and half-wave voltage reveal the conversion efficiency of Mach-Zehnder modulators, which is crucial to the applications such as electro-optic sensing [1–4], fiber-optic gyroscope, [5–7], and arbitrary bias point control [8–10], especially in the low-frequency range. In past decades, there are several time- or frequency-domain methods proposed to measure electro-optic parameters of Mach-Zehnder modulators (MZMs) for low-frequency applications. The most direct power-voltage (P-V) method is to sweep the P-V curve through applying different direct current (DC) voltages on the bias port of the MZM under test [11]. However, it is only efficient for extracting the DC half-wave voltage at the bias port, which is useless for the dynamic half-wave voltage measurement at the modulation port.

Received: 25 October 2022 / Revised: 11 December 2022

DOI: 10.1007/s13320-023-0678-9
Article type: Regular

Alternatively, the triangular-wave method is developed by applying a time-variation triangular-wave voltage either on the modulation or bias port and observing the output sinusoidal waveform with a photodetector and an oscilloscope [12]. However, it suffers from bias drifting and the measured half-wave voltage is a composite value of multiple harmonic tones coming from the triangular waveform, which can be overcome by sinusoidal-wave driving for the single-tone measurement. Nevertheless, the major difficulty for the time-domain methods lies in that the swing voltages are required to be near at least twice the half-wave voltage ($>2V_\pi$), which may result in serious thermal drifting or even failure for the half-wave voltage measurement [1, 13].

In contrast, the frequency-domain methods can be operated with agile driving levels, such as the swept frequency method and the frequency-shifted heterodyne method [14–19]. The swept frequency method is widely used to characterize the relative frequency response of the MZM with the help of an electrical network analyzer (ENA) [14, 16]. However, this method is not applicable for measuring the absolute frequency response. It should be noted that the absolute frequency response parameters including the modulation depth and half-wave voltage are more comprehensive than the relative one since it reveals not only the relative change of the modulation efficiency but also the modulation efficiency itself. For the absolute frequency response measurement, the self-heterodyne scheme is proposed with an acousto-optic modulator (AOM) as an optical frequency shifter [17]. In this scheme, the low-frequency (sub-MHz) modulated optical signal heterodynes with the frequency-shifted optical carrier, which enables testing the sub-MHz frequency response at the cost of tens of MHz (typically 80 MHz) photodetection. Recently, we propose a low-frequency (sub-MHz) detection scheme for extracting the modulation depth and half-wave voltage of MZMs based on two-tone modulation and bias swing [18], which enables high-speed MZM measurement with a low-frequency photodetector. Nevertheless, the two-tone method assumes that the MZM at the two-tone frequencies has the same half-wave voltages, which is not always valid in the low-frequency range due to the acoustic anomalies in $LiNbO_3$ material unless it is below 100 kHz [20]. Besides, the two-tone and bias driving conditions are somewhat redundant in the case of low-frequency MZM measurement.

In this work, we propose a bias-independent inter-modulation method for measuring low-frequency modulation and bias half-wave voltages of MZMs. Our scheme consists of simultaneous sinusoidal modulation over the modulation and bias ports of the MZM under test. The sinusoidal-modulated sidebands heterodyne with each other and generate the desired inter-modulation products after photodetection, which allows extracting both the modulation depth and half-wave voltages for the modulation and bias ports of the MZM. Our method is independent of bias voltages of the MZM because it can be canceled out by carefully choosing the frequency relationship of the sinusoidal modulation. Moreover, the proposed method enables lower swing voltage for measuring both the modulation depth and half-wave voltage of MZMs. The theoretical description is presented as well as experimental demonstration to confirm our method, and the consistency is fully checked for accuracy.

2. Operation principle

As depicted in Fig. 1, an optical carrier with an angular frequency ω_0 is sent to an MZM driven by two sinusoidal signals $v_1(t) = V_1\sin(2\pi f_1 t+\theta_1)$ at the modulation port and $v_2(t) = V_2\sin(2\pi f_2 t+\theta_2)+V_b$ at the bias port. The optical output field after the MZM can be written by

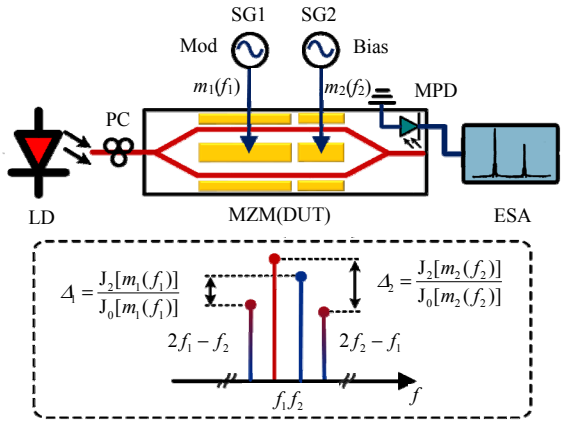

Fig. 1 Schematic diagram of the proposed method. LD: laser diode; PC: polarization controller; MPD: monitor photodetector; Mod: modulation; SG: sinusoidal-function generator; ESA: electrical spectrum analyzer.

$$E_{\mathrm{MZM}}(t) = A_0 \mathrm{e}^{\mathrm{j}\omega_0 t}\cdot\left[1+\gamma \mathrm{e}^{\mathrm{j}m_1\sin(2\pi f_1 t+\theta_1)+\mathrm{j}m_2\sin(2\pi f_2 t+\theta_2)+\mathrm{j}\varphi_b}\right] \quad (1)$$

where A_0 is the amplitude of the optical carrier, γ is the asymmetric factor of the MZM, φ_b is the phase bias from the bias voltage V_b, and m_1 and m_2 are the modulation depths introduced by $v_1(t)$ and $v_2(t)$ and can be expressed by

$$m_1=\pi V_1/V_{\pi 1},\quad m_2=\pi V_2/V_{\pi 2} \quad (2)$$

where $V_{\pi 1}$ and $V_{\pi 2}$ are the half-wave voltages of the modulation port and the bias port, respectively. After photodetection, the modulated optical signal can be converted into a photocurrent and given by

$$i(t)=R\left|E_{\mathrm{MZM}}(t)\right|^2 = RA_0^2\cdot\left\{1+\gamma^2+2\gamma\cos\left[\begin{array}{l} m_1\sin(2\pi f_1 t+\theta_1) \\ +m_2\sin(2\pi f_2 t+\theta_2)+\varphi_b\end{array}\right]\right\} \quad (3)$$

with the responsivity R of the photodetector. Applying the Jacobi-Anger expansion to (3), it can be expressed as

$$i(t)=RA_0^2\left\{\begin{array}{l} 1+\gamma^2+ \\ 2\gamma\sum\limits_{p=-\infty}^{+\infty}\sum\limits_{q=-\infty}^{+\infty}\mathrm{J}_p(m_1)\mathrm{J}_q(m_2)\cdot \\ \cos\left[2\pi p f_1 t+2\pi q f_2 t+p\theta_1+q\theta_2+\varphi_b\right]\end{array}\right\} \quad (4)$$

where $\mathrm{J}_p(\cdot)$ and $\mathrm{J}_q(\cdot)$ are the pth and qth-order Bessel functions of the first kind, respectively. From (4), the desired frequency components can be quantified as follows:

$$i(f_1)=2\gamma A_0^2 R(f_1)\mathrm{J}_0(m_2)\mathrm{J}_1(m_1)\sin(\varphi_b) \quad (5a)$$

$$i(f_2)=2\gamma A_0^2 R(f_2)\mathrm{J}_0(m_1)\mathrm{J}_1(m_2)\sin(\varphi_b) \quad (5b)$$

$$i(2f_2-f_1)=2\gamma A_0^2 R(2f_2-f_1)\mathrm{J}_2(m_2)\mathrm{J}_1(m_1)\sin(\varphi_b) \quad (5c)$$

$$i(2f_1-f_2)=2\gamma A_0^2 R(2f_1-f_2)\mathrm{J}_2(m_1)\mathrm{J}_1(m_2)\sin(\varphi_b). \quad (5d)$$

It can be seen from (5b) and (5d) that the frequency components at $2f_1-f_2$ and f_2 have the same amplitude factor of $2\gamma A_0^2\mathrm{J}_1(m_2)\sin(\varphi_b)$. In our method, the two frequencies f_1 and f_2 are set very close to each other to let the assumption on the responsivity $R(2f_1-f_2)\approx R(f_2)$ stand. In this case, the modulation depth m_1 can be extracted from the relative amplitude between the frequency components at $2f_1-f_2$ and f_2, given by

$$H_1(m_1)=\frac{i(2f_1-f_2)}{i(f_2)}=\frac{\mathrm{J}_2(m_1)}{\mathrm{J}_0(m_1)}. \quad (6)$$

Similarly, with (5a) and (5c), the modulation depth m_2 can also be extracted from the relative amplitude between the frequency components at $2f_2-f_1$ and f_1, given by

$$H_2(m_2)=\frac{i(2f_2-f_1)}{i(f_1)}=\frac{\mathrm{J}_2(m_2)}{\mathrm{J}_0(m_2)}. \quad (7)$$

It is also worth noticing that our measurement only depends on the relative amplitude instead of the absolute amplitude of the desired frequency components from (6) and (7), which eliminates the effect from the power fluctuation of the laser diode (LD) and the uneven responses of photo-diodes. Moreover, the frequency response measurement of modulation and bias ports can be realized simultaneously and independently. Besides, the measurement is independent of the bias voltage of the MZM. In practice, it will benefit from an improved signal-to-noise ratio (SNR) by setting a relatively high signal driving level and a near quadrature bias phase.

3. Results and discussion

In our experiment, an optical carrier at the wavelength of 1550.12 nm is injected into the MZM (iXblue MXER-LN-10) via a polarization controller. The low-frequency driving signals come from a dual-channel function generator (Hantek HDG2102B) applied to the modulation and bias ports of the MZM, respectively, working as an inter-modulation of the optical carrier. The bias phase φ_b is adjusted through the bias voltage V_b of the MZM. The output signal is detected by the onsite MPD and analyzed by an electrical spectrum analyzer (ESA).

As can be seen from Fig. 2(a), the low-frequency electrical power of the modulation and bias-modulated components are detected at f_1, f_2, $2f_1 - f_2$, and $2f_2 - f_1$, respectively, in which the frequencies are set as $f_1 = f_2 - 10$. For example, when the frequencies of f_1 and f_2 are set to be 1kHz and 1.01 kHz, the values of the electrical power at desired frequency components of 1 kHz (f_1), 1.01 kHz (f_2), 0.99 kHz ($2f_1 - f_2$), and 1.02 kHz ($2f_2 - f_1$) are measured to be –43.46 dBm, –46.66 dBm, –67.31 dBm, and –70.20 dBm, respectively. The amplitude of the driving signal is determined to be 2.25 V (17.04 dBm) at 1.01 kHz. According to (6), the modulation depth m_1 of the modulation port at 1 kHz is solved to be 1.63 rad. Therefore, the half-wave voltage $V_{\pi 1}$ is calculated to be 4.35 V based on (2). Similarly, the modulation depth m_2 and half-wave voltage $V_{\pi 2}$ of the bias port at 1.01 kHz are also determined to be 1.18 rad and 5.98 V, respectively. And Fig. 2(b) shows the measured typical electrical spectra at f_1 (10 kHz), f_2 (10.01 kHz), $2f_1 - f_2$ (9.99 kHz), and $2f_2 - f_1$ (10.02 kHz) after photodetection.

In order to verify the bias independence of the proposed method, the absolute and relative electrical power of the desired frequency components at different bias voltages in the case of 10 kHz (f_1), 10.01 kHz (f_2), 9.99 kHz ($2f_1 - f_2$), and 10.02 kHz ($2f_2 - f_1$) are measured, respectively, as shown in Fig. 3. From Fig. 3, although the absolute electrical power varies with the bias voltage V_b, the relative power in between almost keeps constant as long as the SNR of the desired frequency

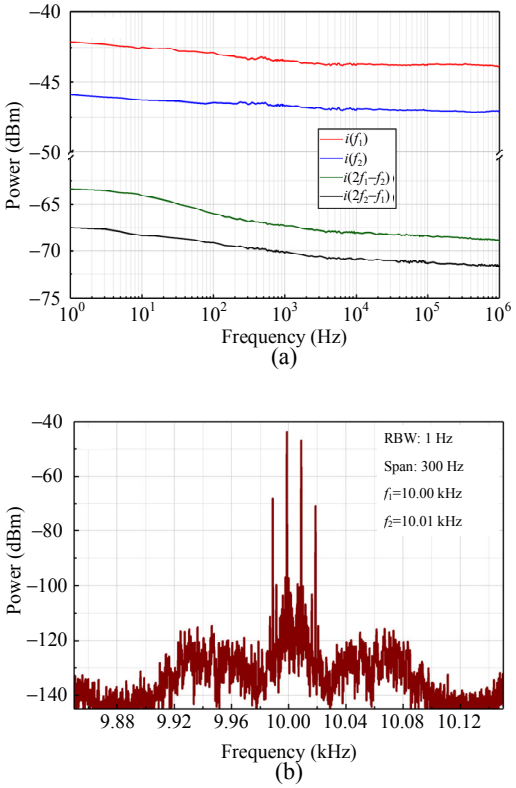

Fig. 2 Measured electrical power and spectra: (a) electrical power of the electrical signals after photodetection at f_1, f_2, $2f_1 - f_2$, and $2f_2 - f_1$ and (b) electrical spectrum in the case of f_1 = 10 kHz and f_2 = 10.01 kHz.

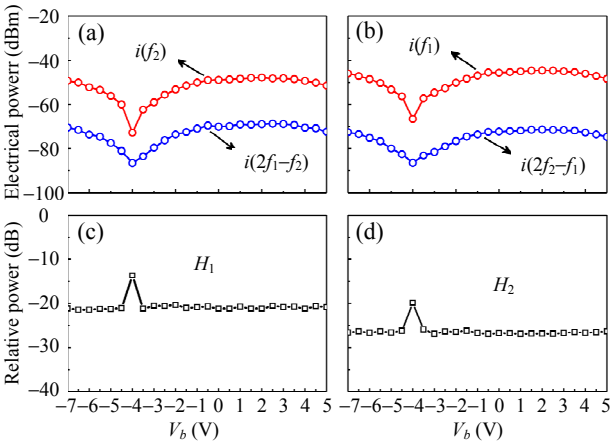

Fig. 3 Measured electrical power at different bias voltages: electrical power at (a) f_2, $2f_1 - f_2$ and (b) f_1, $2f_2 - f_1$, corresponding relative power (c) H_1 and (d) H_2 in the case of f_1 = 10 kHz and f_2 = 10.01 kHz.

components can be guaranteed. It is worth noting that weak signals with the poor SNR should be avoided as much as possible in the experiment because they will result in unexpected errors or even failure for the half-wave voltage measurement. The bias independence can be explained by (5a), (5b), (5c), and (5d), and the relative amplitude between the two desired frequency components is independent of varying the bias voltages as the bias phases contribute equally to the absolute amplitudes. Therefore, our method allows measuring the frequency response without specially pre-optimizing the bias characteristics of the MZM.

The modulation depths of the modulation port and bias port are measured at other frequencies according to (6) and (7), as illustrated in Fig. 4. The according half-wave voltages are acquired and shown in Fig. 5. In order to demonstrate the accuracy of the proposed method, we make a comparison between the proposed method and the sinusoidal-wave method for the measurement of half-wave voltages at the modulation and bias ports of the MZM, respectively. As shown in Fig. 5, the experimental results have an excellent consistency between our method and the sinusoidal-wave method. In Fig. 5, it is noted that the sinusoidal-wave method is not qualified for the measurement at above hundreds of kHz due to the non-negligible phase drift and the thermal effects resulting from the large swing voltage [1]. Superior to the sinusoidal-wave method, our method allows simultaneous implementation of the modulation and bias ports measurement while avoiding the effects of the large signal driving level requirements in the low-frequency range. Moreover, as can be seen from Fig. 5, the measurement frequency range in our method can be extended to a lower frequency range (below 1 Hz) with a lower minimum operating frequency of the dual-channel function generator and ESA.

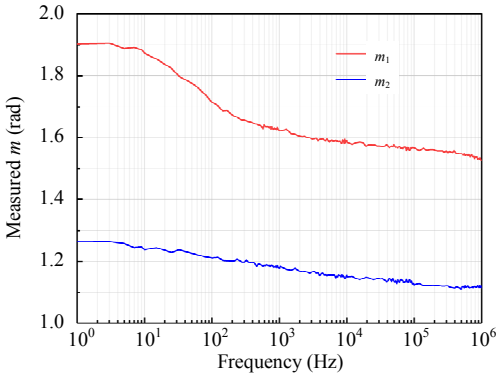

Fig. 4 Measured modulation depths of modulation and bias ports of the MZM as a function modulation frequency, where the microwave driving level is set to be 2.25 V (17.04 dBm).

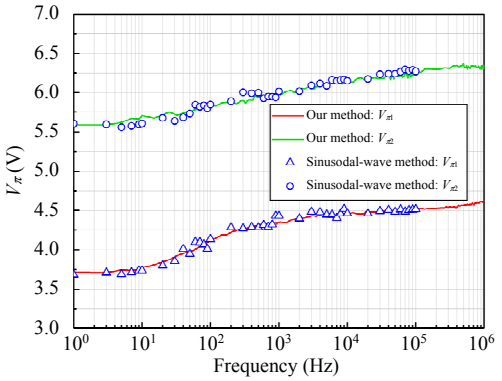

Fig. 5 Measured half-wave voltages with our method and the sinusoidal-wave method.

4. Measurement uncertainty

For completeness, the measurement uncertainty of the proposed method is also studied by deriving the total differential of (2), (6), and (7), which is expressed as

$$\frac{\delta V_{\pi i}}{V_{\pi i}} = \frac{\delta V_i}{V_i} - \frac{\delta m_i}{m_i} \quad , \quad i = 1,\ 2 \tag{8}$$

and

$$\frac{\delta m_i}{m_i} = F \frac{\delta H(m_i)}{H(m_i)} \tag{9}$$

with the error transfer factor F, given by

$$F = \frac{\mathrm{d}m_i / m_i}{\mathrm{d}H / H} = \frac{\mathrm{J}_0(m_i)\mathrm{J}_2(m_i)}{m_i \mathrm{J}_1(m_i)\mathrm{J}_2(m_i) + m_i \mathrm{J}_0(m_i)\mathrm{J}_1(m_i) - 2\mathrm{J}_0(m_i)\mathrm{J}_2(m_i)}. \tag{10}$$

As shown in Fig. 6, the error transfer factor F is less than 0.6 in the case of $0 < m < 4$ and even can be reduced to 0 as long as the modulation depth m is 2.4 rad, indicating that the uncertainty of the extracted modulation depth will be less than that of the measured relative amplitude function. In our experiment, the measurement error is mainly caused by the uneven responsivity of the MPD due to the approximation of $R(f_2 - 2f_1) \approx R(f_2)$ and the uncertainty of the ESA. The responsivity difference of the MPD is estimated to be no more than 0.1 dB within a 10 Hz frequency difference, and the power measurement uncertainty is estimated to be within 0.1 dB from the ESA specification. Therefore, the measured relative amplitude H would have an uncertainty of less than 0.3 dB (= 0.1 + 2 × 0.1), which means a relative error introduced by the MPD and ESA less than 3.51% [$F \cdot \delta H(m)/H(m) \leq (10^{0.3/20} - 1) \times 100\%$]. It should be noted that the relative error can be further improved with the high-performance PD and ESA. Besides, the driving level difference is estimated to be less than [1% + (1 mV/V_{set}) × 100%] based on the function generator specification, corresponding to an uncertainty of 1.04% [1% + (1/2250) × 100%]. Of note, V_{set} is the peak voltage output from the function generator. In total, the measured modulation depth is estimated to have an uncertainty of less than 4.55% (3.51% + 1.04%).

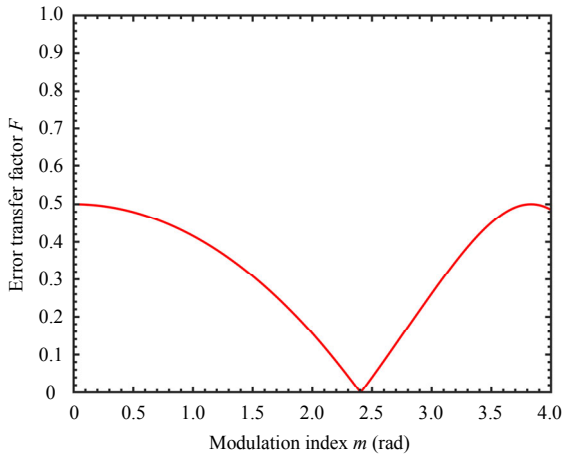

Fig. 6 Error transfer factors.

5. Conclusions

In summary, we have proposed and demonstrated a bias-independent method for simultaneously measuring the low-frequency modulation and bias half-wave voltage of MZMs based on the inter-modulation. Different from the electro-optic swept frequency method [15, 16], the proposed method enables the absolute frequency response measurement of MZMs at the low-frequency range. Compared with the sinusoidal-wave method and triangular-wave method [12], the proposed method enables the bias-independent measurement of the modulation depth and half-wave voltage for both the modulation and bias ports, and avoids any strict swing amplitude requirement. Superior to the frequency-shifted heterodyne method [21–23], the method eliminates the limitation of the low-frequency characterization of MZMs based on the inter-modulation. Therefore, our method provides the high-resolution absolute frequency response measurement for MZMs, leading a bias-drift-free electrical measurement with the high accuracy ranging from 1 Hz to 1 MHz.

Acknowledgment

This work was supported in part by the National Natural Science Foundation of China (Grant No. 61927821); National Key Research and Development Program of China (Grant No. 2018YFE0201900); Fundamental Research Funds for the Central Universities (Grant No. ZYGX2019Z011).

References

[1] T. Ichikawa, M. Kagami, O. Watanabe, M.

Tsuchimori, and H. Ito, "Very-low-frequency response of a nonlinear urethane-urea copolymer optical modulator," *Japanese Journal of Applied Physics*, 2002, 41(3A): L243–L245.

[2] M. Q. Ren, P. Lu, L. Chen, and X. Y. Bao, "Study of *Φ*-OTDR stability for dynamic strain measurement in piezoelectric vibration," *Photonic Sensors*, 2016, 6(3): 199–208.

[3] A. L. Ricchiuti, D. Barrera, S. Sales, L. Thevenaz, and J. Capmany, "Long fiber Bragg grating sensor interrogation using discrete-time microwave photonic filtering techniques," *Optics Express*, 2012, 21(23): 28175–28181.

[4] W. Sun, X. Y. Liu, and M. Deng, "High-precision magnetic field sensor based on fiber Bragg grating and dual-loop optoelectronic oscillator," *Photonic Sensors*, 2022, 12(4): 220419.

[5] W. Wang, J. L. Xia, and Y. X. Xu , "Research on integrated optical gyroscope," in *2008 2nd International Symposium on Systems and Control in Aerospace and Astronautics (ISSCAA).IEEE*, China, 2008, pp. 4776343.

[6] D. N. Liu, H. Li, X. Wang, H. L. Liu, P. R. Ni, N. Liu, and L. S. Feng, "Interferometric optical gyroscope based on an integrated silica waveguide coil with low loss," *Optics Express*, 2020, 28(10): 15718–15730.

[7] P. P. Khial, A. D. White, and A. Hajimiri, "Nanophotonic optical gyroscope with reciprocal sensitivity enhancement," *Nature Photonics*, 2018, 12: 671–675.

[8] S. Aisawa, H. Miyao, N. Takachio, and S. Kuwano, "DC drift compensation method using low frequency perturbation for $LiNbO_3$ intensity modulator," in *Technical Digest CLEO/Pacific Rim '97 Pacific Rim Conference on Lasers and Electro-Optics, IEEE*, Japan, 1998, pp. 123–124.

[9] Y. P. Li, Y. A. Zhang, and Y. Q. Huang, "Any bias point control technique for Mach-Zehnder modulator," *IEEE Photonics Technology Letter*, 2013, 25(24): 2412–2415.

[10] Z. Y. Pan, S. F. Liu, N. Zhu, P. Li, M. Z. Liu, L. Yang, *et al.*, "Arbitrary bias point control for Mach-Zehnder modulator using a linear-frequency modulated signal," *IEEE Photonics Technology Letter*, 2021, 33(11): 577–580.

[11] P. Cross, R. Baumgarner, and B. Kolner, "Microwave integrated optical modulator," *Applied Physics Letters*, 1984, 44(5): 486–488.

[12] R. A. Becker, "Traveling wave electro optic modulator with maximum bandwidth length product," *Applied Physics Letters*, 1984, 45(11): 1168–1170.

[13] S. Sun, M. He, M. Xu, S. Gao, Z. Chen, X. Zhang, *et al*., "Bias-drift-free Mach-Zehnder modulators based on a heterogeneous silicon and lithium niobate platform," *Photonics Research*, 2020, 8(12): 1958–1963.

[14] S. G. Uehara, "Calibration of optical modulator frequency response with application to signal level control," *Applied Optics*, 1978, 17(1): 68–71.

[15] P. D. Hale and D. F. Williams, "Calibrated measurement of optoelectronic frequency response," *IEEE Transactions on Microwave Theory and Techniques*, 1993, 51(4): 1422–1429.

[16] X. M. Wu, J. W. Man, L. Xie, J. G. Liu, Y. Liu, and N. H. Zhu, "A new method for measuring the frequency response of broadband optoelectronic devices," *IEEE Photonics Journal*, 2012, 4(5): 1679–1685.

[17] K. Toki, M. Yoshikawa, D. Uesaka, H. Toda, H. Iwata, T. Kawanishi, *et al.*, "Frequency response measurement of half-wave voltage and chirp parameter of $LiNbO_3$ intensity modulators in low frequency range," in *2011 International Topical Meeting on Microwave Photonics jointly held with the 2011 Asia-Pacific Microwave Photonics Conference (MWP/APMP)*, Japan, 2011, pp. 354–356.

[18] S. J. Zhang, C. Zhang, H. Wang, X. H. Zou, Y. Liu, and J. E. Bowers, "Calibration-free measurement of high-speed Mach-Zehnder modulator based on low-frequency detection," *Optics Letters*, 2016, 41(3): 460–463.

[19] M. Yoshioka, S. Sato, and T. Kikuchi, "A method for measuring the frequency response of photodetector modules using twice-modulated light," *Journal of Lightwave Technology*, 2005, 23(6): 2112–2117.

[20] R. L. Jungerman and C. A. Flory, "Low-frequency acoustic anomalies in lithium niobate Mach-Zehnder interferometers," *Applied Physics Letters*, 1988, 53(16): 1477–1479.

[21] S. J. Zhang, C. Zhang, H. Wang, Y. Liu, J. D. Peters, and J. E. Bowers, "On-wafer probing-kit for RF characterization of silicon photonic integrated transceivers," *Optics Express*, 2017, 25(12): 13340–13350.

[22] S. J. Zhang, C. Zhang, H. Wang, X. H. Zou, Y. L. Zhang, Y. Liu, *et al*., "Self-calibrated microwave characterization of high-speed optoelectronic devices by heterodyne spectrum mapping," *Journal of Lightwave Technology*, 2017, 35(10): 1952–1961.

[23] Y. Xu, S. J. Zhang, X. H. Zou, Z. T. Ruan, Y. T. He, H. P. Li, *et al*., "Characterization of high-speed electro-optic phase modulators based on heterodyne carrier mapping at a fixed low-frequency," *Optics Express*, 2023, 31(2): 1656–1665.